Research Square

Preprints are preliminary reports that have not undergone peer review.
They should not be considered conclusive, used to inform clinical practice,
or referenced by the media as validated information.

Glycolysis is critical to sperm hyperactivation and oxidative phosphorylation is supportive

Manorma Dixit
CSIR-Central Drug Research Institute
Prashansa Khanna
CSIR-Central Drug Research Institute
Bidhan Chandra Nayak
CSIR-Central Drug Research Institute
Sudesh Kumar Banyal
CSIR-Central Drug Research Institute
Radha Rangarajan
CSIR-Central Drug Research Institute
Rajender Singh
rajender.singh.cdri@csir.res.in

CSIR-Central Drug Research Institute

Research Article

Keywords: non-hormonal contraception, sperm motility, sperm fertility, hyperactivation

Posted Date: June 12th, 2026

DOI: https://doi.org/10.21203/rs.3.rs-9916063/v1

License: This work is licensed under a Creative Commons Attribution 4.0 International License.
Read Full License

Additional Declarations: No competing interests reported.

Glycolysis is critical to sperm hyperactivation and oxidative phosphorylation is supportive

Manorma Dixit[1#], Prashansa Khanna[1#], Bidhan Chandra Nayak[1], Sudesh Kumar Banyal[1], Radha Rangarajan[1,2], Rajender Singh[1,2]*

#equal contribution

1 CSIR-Central Drug Research Institute, Lucknow, Uttar Pradesh, India

2 Academy of Scientific and Innovative Research (AcSIR), Ghaziabad, Uttar Pradesh, India

***Corresponding author**

Dr. Rajender Singh

Division of Endocrinology

Central Drug Research Institute, Lucknow, India

E-mail: rajender_singh@cdri.res.in

Phone No. 522-2612411-18 Extn. 4393

Fax: +91-522-2771941

Abstract

Background: Human sperm traverse a long distance from the site of ejaculation to the site of fertilization, making it an energy intensive process. In the present study, we asked if glycolysis is critical to human sperm fertility which can make it an attractive target for achieving non-hormonal contraception by blocking sperm motility.

Methods: Semen samples from normozoospermic fertile donors were used for experimental testing. Sperm were washed and incubated in different energy substrate media followed by sperm kinematic analysis. Further, glycolysis and OXPHOS were inhibited using specific inhibitors to corroborate findings from substrate depletion experiments. ATP levels were measured using the ATP assay kit and the glycolytic and oxphos ATP production rates were estimated using the Seahorse assay.

Results: Substrate depletion experiments showed that intracellular energy reserves were sufficient to sustain basal sperm motility for several hours; however, exogenous glucose was essential for sperm hyperactivation. In line with this, blocking glucose uptake under physiological conditions with 2-deoxyglucose (2-DG) resulted in a near-complete loss of hyperactivation. In parallel, the inhibition of OXPHOS using specific inhibitors (oligomycin, rotenone, antimycin A, or FCCP) significantly reduced sperm motility and hyperactivation, indicating a substantial contribution of mitochondrial respiration under starving conditions. However, OXPHOS inhibition alone failed to markedly suppress hyperactivation under physiological conditions.

Conclusion: The study suggests a critical requirement of exogenous glucose/glycolysis in achieving sperm hyperactivation.

Keywords: non-hormonal contraception, sperm motility, sperm fertility, hyperactivation

Background

Human spermatozoa must swim approximately 3,000 times their own length in the female reproductive tract (FRT) to reach the site of fertilization, a process that requires a substantial amount of energy. Consequently, targeting sperm function within the FRT represents an attractive strategy for non-hormonal contraception. Among currently explored sperm-specific targets, soluble adenylyl cyclase and ion channel proteins have gained prominence because their inhibition can rapidly immobilize spermatozoa in the FRT [1,2]. Additional promising targets include proteins involved in sperm–oocyte interaction and fertilization [3,4]. In contrast, energy-producing enzymes remain a relatively underexplored target class for contraception. One major challenge is the pronounced species-specific variability in sperm energy metabolism, as different species preferentially utilize distinct substrates. For instance, capacitation requires glucose in mice [5], oxidizable substrates such as pyruvate and lactate in bulls and stallions [6,7], and a combination of glycolytic and oxidative phosphorylation (OXPHOS) substrates in humans [8–11]. Despite the availability of oxygen, mammalian sperm preferentially rely on glycolysis, underscoring its critical role in male fertility [10,12]. Consistent with this, seven mouse knockout models targeting glycolytic enzymes (HK1S, ALDOART2, GAPDHS, PGK2, ENO4, PKM, and LDHC) have been generated. Of these, five resulted in infertility [13–17], one remained fertile (ALDOART2) [18], and one was subfertile (PGK2) [19]. These findings support the concept that inhibition of glycolysis could be an effective strategy for contraception. However, the pronounced interspecies differences in sperm metabolism and the lack of known/validated mutations in genes involved in glycolysis in humans, complicate the translation of animal data, emphasizing the necessity for direct experimentation on human sperm to identify optimal targets for disrupting energy production in the context of non-hormonal contraception.

Spermatozoa encounter a series of highly diverse environments during their journey to the site of fertilization. The first major barrier encountered by sperm in the FRT is cervical mucus, which selectively filters out poor-quality spermatozoa while permitting the passage of those with superior motility and morphology [20,21]. Concurrently, sperm undergo the prolonged and tightly regulated process of capacitation, through which they acquire the ability to undergo hyperactivated motility [22,23]. Following this, sperm traverse the uterine–tubal junction (UTJ) to enter oviducts, where they can remain viable and metabolically active for up to 5-7 days, awaiting oocyte arrival [24,25]. Sperm achieve hyperactivation in the FRT, enabling the cumulus cell matrix penetration, followed by zona pellucida penetration through specific sperm–oocyte protein interactions [22,23,26]. Fertilization culminates with fusion of the sperm plasma membrane with the oocyte membrane, initiating embryonic development. Each of these sequential processes are highly energy intensive, requiring precisely timed and localized ATP production to sustain both progressive and hyperactivated motility [8]. Collectively, these observations highlight sperm energy metabolism as an attractive target for contraceptive intervention. However, it remains unclear which specific metabolic pathways could be targeted to reliably and reversibly impair human sperm function, underscoring a critical gap in our understanding relevant to the development of non-hormonal contraception.

In this study, we investigated the role of energy metabolism in human sperm using two complementary approaches: substrate depletion and pharmacological inhibition of specific enzymes involved in glycolysis and oxidative phosphorylation (OXPHOS). In the first phase, human sperm were exposed to defined combinations of energy substrates, and the resulting effects on sperm motility were quantified. These conditions included glucose, pyruvate, and lactate, alone or in combination, at concentrations relevant to the female reproductive tract (FRT). In the second

phase, we employed inhibitors targeting glycolytic and OXPHOS pathways to assess their effects on sperm motility in a physiologically relevant medium (human tubal fluid, HTF). To corroborate these findings, we performed intracellular ATP measurements and Seahorse metabolic flux analyses, providing deeper insights into how substrate availability and pathway inhibition influence ATP production in human sperm.

Materials and methodology

Reagents and Media

All general chemicals were procured from Sigma-Aldrich (USA) unless otherwise indicated. Oligomycin & Rotenone-Antimycin A were used from the Agilent Seahorse real time ATP Assay kits. Human Tubal Fluid (HTF) medium was used for in vitro capacitation of sperm. Firstly, we prepared the HTF basal medium, which included $CaCl_2 \cdot 2H_2O$ (2.04 mM), NaCl (101.6 mM), KCl (4.69 mM), $MgSO_4 \cdot 7H_2O$ (0.2 mM), KH_2PO_4 (0.37mM), $NaHCO_3$ (25 mM), phenol red (0.002 g/L), penicillin (0.075 g/L) and streptomycin (0.05 g/L). This was further supplemented with BSA (4 mg/mL) after adjusting pH to 7.4. Then, we added energy substrates, glucose (2.78 mM), sodium lactate (21.4 mM), and sodium pyruvate (0.33 mM) in different combinations to the basal HTF medium. We used in total six media combinations, GLP (glucose, lactate, pyruvate), GL (glucose, lactate), GP (glucose, pyruvate), LP (lactate, pyruvate), G (glucose only) and O (no substrate). For the Seahorse assay, we used modified PBS containing KCl (2 mM), $MgCl_2$ (0.5 mM), $CaCl_2.2H_2O$ (0.9 mM), and BSA (4 mg/mL), pH 7.4. Before use, all media were equilibrated at 37 °C with 5% CO_2. This way all sperm kinematics assays were performed under capacitating conditions with varying presence of energy substrates.

Sperm Preparation

Semen samples were obtained by masturbation from normozoospermic donors aged 25-45 years after 3-5 days of abstinence, following the WHO guidelines. Donors were proven fertile, had normozoospermic profile at present which was verified before recruiting them in the study. Semen samples were allowed to liquefy at 37 °C for 30 minutes. Liquefied semen samples (3-6 in number) were pooled for further experimentation. Motile sperm were separated by the swim-up method, where 1.2 ml of 'O' medium was gently layered on top of 1 ml semen sample in a 15 ml falcon tube and incubated for one hour at 37 °C with 5% CO_2. After one hour, 1 ml of the top layer of 'O' medium was gently transferred to a microcentrifuge tube and sperm were pelleted by centrifugation at 300 g for 5 minutes. This was followed by washing with 'O' medium at 300 g for 5 minutes. After washing, cells were resuspended in respective medium in 12 well plates to a final concentration of ~10×10^6 cells/mL, counted using Mackler chamber, for 30 minutes at 37 °C with 5% CO_2 to allow maximum motility gain by spermatozoa. All the experimental readings were taken after this 30-minute equilibration of sperm motility, which makes it about 2.5 hours post ejaculation.

Computer-Assisted Sperm Analysis (CASA)

After 30-minute equilibration, cells were incubated at 37 °C with 5% CO_2 for 60 minutes and sperm motility was evaluated every 10 minutes using the Computer Assisted Sperm Analyzer (Hamilton Thorne IVOS II, version 1.17.1. Beverly, USA). All the recordings were taken at the standard instrument settings of 60 frames/s at 37 °C using a temperature-controlled stage, analyzing at least 200 sperm per sample. Sperm parameters recorded for these experiments included total sperm motility (%), progressive motility (%), and hyperactivated motility (%). In addition, CASA also recorded fine sperm motility parameters, including VCL, VSL, VAP, LIN,

STR, WOB, ALH, and BCF. Progressive motility was characterized by STR ≥ 80% and VAP ≥ 25 μm/s, and hyperactivated motility was characterized by VAP >50 μm/s, STR >80%, VCL ≥ 150 μm/s, LIN ≤ 50%, ALH ≥ 7 μm [27].

Vitality Assay

Sperm vitality was analyzed using the Eosin-Nigrosin Staining method according to the WHO 2021 guidelines [28]. The stain was prepared by mixing 1% Eosin and 10% Nigrosin in 1:3 ratio. Equal volume of the staining mixture and sperm samples were mixed and smeared on a clean glass slide, left to dry for 15 minutes and observed under a bright-field microscope. For every sample, 200 spermatozoa were counted including the dead (pink head) and live (unstained head) sperm to calculate the percentage vitality. Starting at the 1st minute, vitality was assessed every 10 minutes in a manner similar to sperm motility measurement.

ATP Measurement

ATP levels were determined with the Abcam (UK) ATP Assay kit (Cat no. ab83355) using fluorescence channel of FLUOstar Omega reader (BMG Labtech, USA). Sperm preparation was undertaken the same way as mentioned above, except that the final concentration was set to 20 × 10^6 for all experimental conditions. Following this, sperm were incubated at 37°C in 5% CO_2 for one hour in the respective medium and inhibitors. Afterwards, sperm were washed once with chilled PBS by centrifugation at 10,000 g for 5 min at 4°C to remove all components of the HTF buffer. The cell pellet was dissolved in the ATP assay buffer and then lysed by adding 5% TCA and incubated for 5 minutes in ice followed by adjustment of pH using KOH. The lysed cells were centrifuged at 10,000 g for 5 min at 4°C to remove the pellet and the clear supernatant was transferred into a fresh tube. ATP assay reaction mixture was prepared according to the

manufacturer's protocol. The supernatant was added to the reaction mixture and incubated at room temperature for 30 minutes. Following this, the fluorescence was measured at 535/587 nm in duplicates. ATP concentration (nmol/µl) for 20 million sperm was calculated using fluorescence readings according to the ATP standard curve generated using kit components and suggested protocol.

Seahorse Assay

ATP production rate of human spermatozoa was quantified using the Agilent Seahorse XFe24 analyzer (USA). The sensor cartridges, cell culture plates, calibrant solution (FluxPak, Cat no. 102340-100) and assay compounds (real time ATP assay kit, Cat no.103592-100) were procured from Agilent technologies. One day prior to conducting the assay, the sensor cartridge was hydrated with the calibrant solution and the cell culture plate wells were coated with 25µL of 0.5 mg/mL Concanavalin A (conA) and incubated overnight at 37°C and room temperature, respectively. The sperm cells were prepared as described above. After equilibration of sperm motility, cells were incubated for one hour in various compositions of the HTF medium at 37°C with 5% CO_2. After this incubation, sperm were washed with modified PBS to remove HTF components as bicarbonates in the HTF buffer would interfere with the effective extracellular acidification rate (ECAR) measurements during the assay. Finally, the cells were suspended in the same modified PBS with respective energy substrates for loading in the 24 well Seahorse cell culture plate. In case of inhibitors, compounds (10mM 2-DG and 50mM sodium oxamate) were added at this point. The cell suspension was added to the ConA coated wells (500µL/well) at a final cell count of ~6 million per well. To adhere the sperm heads to the concanavalin A coated surface, the Xfe24 cell culture plate was centrifuged at 200 *g* for one min at the lowest breaking speed. Thereafter, the cell plate was turned 180 degrees and centrifuged again with the same

parameters for uniform distribution of cells. We confirmed the uniform distribution and attachment of sperm head with conA coated plate under the microscope to evaluate exact count and eliminate the possibility of any floating cells in the plate, so that there are no further biochemical assays required to confirm cell density. The plate was then incubated at 37 ℃ in non-CO_2 incubator for 30 min, before starting the analysis to firmly attach cells. Meanwhile, the port A and B of the hydrated sensor cartridge plate were loaded with Oligomycin (1.5 µM/well) and Rotenone Antimycin A (0.5 µM/well), respectively, based on the standard assay protocol, followed by calibration of the cartridge. The standard method of the assay was modified by deleting the equilibration step and changing the mix, wait and measure steps to 1.5, 0.5, and 3 minutes, respectively with 3 cycles per stage. In addition, the buffer factor for this modified PBS based assay buffer was estimated separately (calculated value 2.0, data not shown) and used in the subsequent calculation of the proton efflux rate (PER). After the completion of assay, data was analyzed and normalized to one million cells per well. The calculations for mitochondrial and glycolytic ATP production rates were performed using the Agilent Wave report generator application (version 2.6.4.24).

Statistical analyses

All experiments were repeated between three and eight times. We used GraphPad Prism for statistical analysis and represented the data as Mean + SEM. Each parameter across control and experimental groups were analyzed using paired Student's t-test. A standard p-value of <0.05 was considered statistically significant.

RESULTS

Effects of energy substrates on human sperm motility

Sperm were incubated in media with different substrate compositions to gauge the impact of energy substrate availability on sperm motility. The total motility stayed stable across all groups, with no significant differences between supplemented and un-supplemented conditions (Fig. 1). However, progressive motility varied with the substrate composition. Spermatozoa in the 'O' medium exhibited lowest motility from the beginning, which decreased slightly but gradually over 60 minutes, while all supplemented groups maintained high progressive motility, ranging from 60% to 70% (Fig. 1). Spermatozoa displayed the highest hyperactivation levels in GP and GLP media, reaching 18% and 19% respectively, by 60 minutes. In contrast, GL and G media supported modest hyperactivation of 5% and 3.4%, respectively, whereas, LP and O media did not produce noticeable hyperactivation (Fig. 1). Aligned with these findings, the mean curvilinear velocity (VCL) was significantly higher in sperm incubated in GP, GLP, and GL media, while LP and O media resulted in much lower velocities (Fig. 1).

Sustained effects of energy substrates on sperm motility

To evaluate the long-term effects of energy substrates on sperm performance, motility parameters were assessed up to 24 hours under the same supplementation conditions as described above. Total motility was largely maintained in all supplemented groups, remaining above 80% even after 24 h, whereas spermatozoa in the O medium exhibited a marked time-dependent decline (Fig. 2). Progressive motility, however, showed substrate-specific differences. The best progressive motility was maintained in the GL and GLP media, while in the absence of glucose or pyruvate,

progressive motility started declining after 6 hours. The most significant decline was seen in the O medium, approaching baseline by 24 hours (Fig. 2).

Hyperactivation exhibited the most striking time-dependent variation. At one hour, GP and GLP media supported the highest levels of hyperactivation, but these values declined substantially by 6 hours and were nearly abolished by 24 hours (Fig. 2). In contrast, G and GL conditions induced modest hyperactivation that persisted longer, whereas LP and O failed to sustain significant hyperactivation at any time point. Analysis of curvilinear velocity (VCL) further underscored the role of substrate composition in supporting long-term motility. GL and GLP conditions maintained the highest VCL values up to 18 hours, while GP and G groups showed an early peak followed by a decline after 6 hours. LP and O conditions consistently supported the lowest velocities (Fig. 2). Together, these data demonstrate that while glucose, lactate, and pyruvate each contribute to the maintenance of sperm motility, specific combinations distinctly affect the duration of progressive motility and hyperactivation, with GP and G supporting short-term hyperactivation but GL and GLP sustaining velocity over extended periods of time. Sperm remained viable in all media up to at least 24 hours (Supplementary Fig. 1).

Glucose is critical to hyperactivated motility

From the above experiments, it is clear that sperm can remain progressively motile for up to 6 hours even in starving conditions, though hyperactivation cannot be achieved under starving conditions. We next asked if the progressive motility under starving conditions is dependent on glucose. For this, we conducted further experiments in the ‘O’ medium in the presence of 2-DG so that even the internal glucose is not available to the cell. 2-Deoxy-D-Glucose (2-DG), an analogue of glucose competitively inhibits the hexokinase enzyme, blocking the first irreversible

step of glycolysis, yet keeping the cell viable (supplementary Fig. 2). After the addition of 2-DG (10mM and 25mM) [29,30], sperm motility was recorded using CASA every 10 minutes up to 60 minutes. These experiments were conducted under two conditions; starving and physiological, to answer two different questions. Under starving conditions, 2-DG did not affect sperm motility significantly, but reduced progressive motility significantly, suggesting that progressive motility under starving conditions is critically dependent on the intracellular glucose. In complete GLP medium, 2-DG did not affect overall motility, and progressive motility was affected only slightly, but hyperactivation was severely reduced (Fig. 3), suggesting that blockage of glucose access can be used to curtail sperm fertility under physiological conditions.

Intracellular conversion of pyruvate to lactate is necessary to achieve hyperactive motility

Mammalian sperm have been shown to generate major ATP fraction using anaerobic glycolysis even under aerobic conditions. For anaerobic glycolysis to run continuously, the conversion of pyruvate to lactate is must, in order to recycle NAD^+ that gets utilized in the 6^{th} step (conversion of glyceraldehyde 3-phosphate into 1,3-bisphosphoglycerate with help of enzyme glyceraldehyde 3-phosphate dehydrogenase) of glycolysis. To assess the significance of pyruvate to lactate conversion in supporting glycolysis, sperm were incubated with sodium oxamate [a structural analogue of pyruvate that inhibits lactate dehydrogenase (LDH)] in either GLP-supplemented or substrate-free (O) medium at 37 °C with 5% CO_2. Following the addition of sodium oxamate (50mM and 100mM) [10,31], viability (supplementary Fig. 2) and motility parameters were assessed every 10 minutes up to 60 minutes using CASA (Fig. 4).

Inhibition of LDH activity led to a concentration-dependent reduction in sperm motility. Total and progressive motility declined steadily with increasing sodium oxamate concentration in both GLP and O conditions. It was interesting to note that the presence of sodium oxamate was sufficient to

reduce hyperactivation to almost nil even in the complete GLP medium in a manner similar to 2-DG, suggesting critical significance of this step in supporting glycolysis. Consistently, curvilinear velocity (VCL) decreased with sodium oxamate treatment in a dose-dependent manner (Fig. 4). In all these set of experiments, GLP control was able to support higher sperm motility, progressive motility, hyperactivation, and curvilinear velocity in comparison to starving medium. These findings suggest that even if sufficient glucose is available, the conversion of pyruvate to lactate is critical to support hyperactivation.

Sperm motility in the presence of OXPHOS inhibitors

While mammalian sperm are known to utilize anaerobic ways of ATP production despite aerobic conditions, OXPHOS may not be dispensable as ATP generation via OXPHOS is economical and massive. To assess the significance of OXPHOS, we blocked OXPHOS activity using oligomycin (ATP synthase blocker), and inhibitors of the proton pump; antimycin A (mitochondrial complex III blocker), and rotenone (complex I blocker) (Fig. 5). In the presence of complete medium (physiological conditions in FRT), OXPHOS inhibition using oligomycin (1.5μM) and rotenone-antimycin A (0.5μM) [29] (ORA) combination displayed negligible reduction in total motility and progressive motility; however, there was significant decline in the hyperactivated motility, suggesting that OXPHOS contributes to sperm hyperactivation (Fig. 5). In contrast, under starving conditions, OXPHOS inhibition significantly lowered total and progressive motility with almost no hyperactivation, again suggesting that OXPHOS has significant contributions to total motility, progressive motility and hyperactivation under substrate limiting conditions (Fig. 5). Taken together, these findings suggest that sperm are highly dependent on glycolysis; however, OXPHOS appears to play a basal role in cellular metabolism to support motility, progressive motility and hyperactivation.

We also asked the above question using OXPHOS uncoupler, which disconnects ATP synthase from H^+ ion transport across the mitochondrial membrane. In the presence of FCCP (5μM), ATP production by OXPHOS would be severely compromised. FCCP acted in a manner highly similar to ORA, suggesting that OXPHOS plays a supportive role in sperm motility, progressive motility and hyperactivation, and compromising OXPHOS would significantly affect hyperactivation under physiological conditions (Fig. 6). The viability of cells after adding ORA combination and FCCP was checked every 10^{th} minute up to 60 minutes (supplementary Fig. 2).

Total ATP level and ATP production rate under various external energy substrates

Using the fluorescence ATP assay and the Seahorse assay, we quantified the total cellular ATP levels and the real-time ATP production rates from glycolysis and mitochondrial respiration in media containing different combinations of energy substrates, GLP, GL, GP, G, LP and O (nil or starving). Using Abcam ATP assay kit, we observed that most media combinations supported good intracellular ATP levels with slight reduction in the absence of glucose (LP medium). Further, the lack of any external energy substrate reduced the total intracellular ATP levels; however, sperm were able to maintain a good level of ATP (Fig. 7). The availability of significant ATP levels under starving conditions, led us to probe the relative contribution of glycolysis and OXPHOS to ATP production under different media combinations, using the Seahorse ATP assay. We found that G, GP and GLP exhibited highest rates of total ATP production. Media containing glucose (GLP, GL, GP, G) demonstrated higher glycolytic ATP production rates compared to the mitochondrial ATP production rates, which aligns with the fact that human sperm are largely glycolytic in nature. Similar to the total ATP level, the ATP production rate was significantly lower in media lacking glucose (LP and O). Two main observations from this assay were that the presence of glucose significantly increases the glycolytic ATP and under glucose deprivation, sperm tend to switch to

OXPHOS with a slight reduction in the total ATP production rate (Fig. 7). The values of OCR and PER normalized to 10^6 cells depict the basal rates for different combinations of substrates (Supplementary Fig. 3).

Total ATP level and ATP production rate in the presence of glycolytic and OXPHOS inhibitors

Intracellular ATP levels were measured using the protocol mentioned above. 2-DG (10mM) significantly reduced ATP production under starving conditions or with supplements (Fig. 8). Since 2-DG blocks the first step of glycolysis, a significant decline in motility and hyperactive motility in the presence of 2DG correlates with low ATP production. Sodium oxamate (50mM) targets the LDH enzyme (the conversion of pyruvate to lactate), resulting in reduced ATP as compared to the control but not as significant as 2-DG (Fig. 8). Sperm treated with mitochondrial inhibitors ORA (oligomycin 1.5 µM and rotenone-antimycin A 0.5 µM) or uncouplers as FCCP (5 µM) showed reduced ATP in the absence of supplements, but were largely unaffected in the presence of energy supplements (Fig. 8). This suggests that OXPHOS produces ATP that contribute to sperm motility significantly, but glycolysis takes precedence in the presence of glycosylable substrates.

Starving conditions had almost no glycolytic ATP production (Fig. 8). Under starving conditions, treatment with the glycolytic inhibitors (2-DG and sodium oxamate) resulted in significant reduction in mitochondrial ATP production rate perhaps, because of low channeling of pyruvate into the TCA cycle. Glycolytic inhibitors (2-DG and sodium oxamate) also reduced glycolytic ATP production in the GLP medium, but the decrease was much lesser in comparison to the starving conditions. The corresponding OCR and PER values, normalized to 10^6 cells, are shown in supplementary Fig. 4.

Discussion

We found that spermatozoa remained motile under most substrate conditions, including in the absence of exogenous energy substrates. Moreover, sperm maintained progressive motility for several hours in the presence of most energy substrates. Despite their ability to maintain motility under starvation, sperm failed to achieve hyperactivation in the absence of external energy substrates, indicating that exogenous substrates are essential for this process. Further experiments inhibiting glycolysis demonstrated that glucose uptake is required for hyperactivation, with pyruvate providing additional metabolic support. Maximal hyperactivation was observed in glucose–pyruvate (GP) or glucose–lactate–pyruvate (GLP) media. Collectively, these findings indicate that glycolysis is critical for achieving hyperactivation, and that pyruvate enhances this process by supporting glycolytic metabolism. Consistent with these results, previous studies have shown that mammalian sperm primarily generate energy through anaerobic glycolysis even in the presence of oxygen [32], underscoring the essential role of glucose metabolism in supporting sperm hyperactivation.

Hyperactivation is characterized by vigorous, asymmetric beating of the sperm flagellum and metabolically demanding phase of sperm motility that culminates in fertilization [23]. Glycolysis, although energetically less efficient than oxidative phosphorylation (OXPHOS), provides a rapid means of local ATP generation in the sperm flagellum. In spermatozoa, the spatial compartmentalization of energy metabolism, with mitochondria confined to the midpiece and glycolytic enzymes localized along the flagellum, limits the ability of OXPHOS to supply ATP throughout the length of the tail. Moreover, mitochondrial metabolism cannot effectively replenish cytosolic NAD^+ consumed during the sixth step of glycolysis, a requirement for sustaining high

glycolytic flux. To overcome these constraints, spermatozoa rely on a mitochondria-independent mechanism for ATP production within the flagellum. This is achieved through glycolysis coupled with local regeneration of NAD^+ via the conversion of pyruvate to lactate by lactate dehydrogenase. This metabolic adaptation allows sperm to maintain high rates of glycolysis directly within the tail, thereby supporting hyperactivated motility despite limited mitochondrial–cytoplasmic exchange imposed by cellular compartmentalization. Supporting this model, previous studies demonstrated that radioactively labeled pyruvate supplied to spermatozoa was almost entirely converted to lactate without entering the tricarboxylic acid cycle, indicating that the majority of cytoplasmic pyruvate is diverted toward lactate production to regenerate NAD^+ and sustain glycolysis [10].

Another notable observation from this study was that human spermatozoa remained progressively motile for at least 6 hours in the absence of exogenous energy substrates, suggesting the presence of sufficient intracellular energy reserves or ATP to support basal motility. To investigate the metabolic basis of this phenomenon, we employed a range of glycolytic and OXPHOS inhibitors under both substrate-rich and substrate-deprived conditions. In substrate-rich medium, blocking glucose utilization with 2-deoxy-D-glucose (2-DG) resulted in only a modest reduction in total and progressive motility, likely because glucose was present at high concentrations and 2-DG has approximately five fold lower affinity for hexokinase than glucose [33]. Despite this relatively minor effect on basal motility, 2-DG treatment completely abolished hyperactivation (Fig. 3), further reinforcing the idea that hyperactivation requires a very high glycolytic flux and that even partial impairment of glucose entry into glycolysis is sufficient to disrupt this process. This finding also explains the inability of spermatozoa to achieve hyperactivation under starvation conditions. To determine the metabolic source sustaining motility under starvation, we treated spermatozoa

with 2-DG in substrate-free medium and observed a drastic reduction in progressive motility (Fig. 3). This indicates that residual glycolytic activity, likely supported by intracellular carbohydrate reserves, makes a substantial contribution to maintaining progressive motility in the absence of exogenous energy substrates.

As demonstrated in the experiments described above, the presence of glucose alone was insufficient to induce full hyperactivation, whereas the addition of pyruvate markedly enhanced hyperactivation. To further investigate the role of pyruvate in supporting hyperactivated motility, we inhibited the conversion of pyruvate to lactate under nutrient-rich conditions. Notably, even in the presence of abundant exogenous substrates, blocking pyruvate to lactate conversion resulted in a significant reduction in progressive motility and abolished hyperactivation almost completely (Fig. 4), underscoring the critical importance of this metabolic step for sperm motility. These findings provide strong justification for the requirement of pyruvate in achieving hyperactivation and further emphasize that glucose alone cannot support the pinnacle of this process. Mechanistically, inhibition of pyruvate to lactate conversion likely leads to impaired regeneration of NAD^+, resulting in its sequestration in the reduced form (NADH) and consequent slowing of glycolytic flux. Together, these results reinforce the conclusion that efficient glycolysis, sustained by pyruvate-dependent NAD^+ recycling, is essential for maintaining both progressive motility and hyperactivation in human spermatozoa.

Having established the critical role of glycolysis in progressive motility and hyperactivation, we next examined the contribution of oxidative phosphorylation (OXPHOS) to sperm function. Under nutrient-rich conditions, inhibition of OXPHOS using oligomycin and rotenone-antimycin A (ORA) or FCCP caused only a modest reduction in progressive motility but led to a pronounced

decrease in hyperactivation (Fig. 5&6). In contrast to glycolytic inhibition, OXPHOS blockade did not completely abolished hyperactivation, indicating that while hyperactivation is primarily driven by glycolysis, OXPHOS plays a supportive role. Under starvation conditions, however, OXPHOS inhibition resulted in a substantial decline in total motility and progressive motility, with hyperactivation reduced to nearly undetectable levels (Fig. 5&6). This observation highlights a significant contribution of OXPHOS to sustaining sperm motility when exogenous substrates are scarce or unavailable. Importantly, whereas inhibition of glycolysis consistently abolished hyperactivation, inhibition of OXPHOS merely curtailed it, further reinforcing the notion that glycolysis is the principal metabolic requirement for hyperactivation, with OXPHOS providing auxiliary support.

We propose a model in which OXPHOS primarily maintains the basal cellular metabolism, thereby supporting total and progressive motility, while glycolysis—localized to the flagellum—provides rapid and localized ATP production necessary for hyperactivated motility. Inhibition of OXPHOS likely increases the metabolic burden on glycolysis to sustain essential cellular functions, diverting glycolytic ATP away from flagellar propulsion and consequently impairing hyperactivation even under nutrient-rich conditions. Additionally, ATP generated by OXPHOS in the midpiece may diffuse into the flagellum to support motility, with glycolysis amplifying this effect through localized ATP generation along the tail. Comparative analysis under starvation conditions further underscores this metabolic interplay. Blocking glucose utilization under starvation did not affect total motility, significantly reduced progressive motility, and completely abolished hyperactivation, suggesting that residual glycolysis together with OXPHOS can sustain basal motility but are insufficient to support hyperactivation. Conversely, OXPHOS inhibition under starvation allowed for some total and progressive motility but eliminated hyperactivation,

indicating a metabolic shift toward greater reliance on OXPHOS to support basal and progressive motility. Nonetheless, across all conditions tested, hyperactivation remained critically dependent on glycolysis, with OXPHOS providing supportive input by maintaining basal metabolism and potentially contributing ATP to the flagellum.

Spermatozoa were able to maintain sufficient intracellular ATP levels in the presence of various exogenous energy substrates (Fig. 7), consistent with the lack of significant changes in total and progressive motility across different substrate conditions. In contrast, starvation led to a significant reduction in cellular ATP levels, which correlated with the observed decrease in progressive motility under these conditions. Importantly, however, hyperactivation is not determined by absolute ATP levels but rather by the rate of ATP production [23,34]. Inhibition of glycolysis with 2-deoxy-D-glucose (2-DG) resulted in a marked reduction in ATP levels, whereas inhibition of pyruvate to lactate conversion with sodium oxamate did not significantly decrease ATP levels (Fig. 8), despite its pronounced inhibitory effect on progressive motility. Notably, sodium oxamate reduced hyperactivation to a similar extent as 2-DG upon starvation, likely due to its impact on ATP production rates, as revealed by Seahorse metabolic analysis. Likewise, the inhibition of OXPHOS with oligomycin and rotenone-antimycin A (ORA) or FCCP did not significantly reduce ATP levels under nutrient-rich conditions (Fig. 8), consistent with their modest effects on total and progressive motility in these conditions. Under starving conditions, however, inhibition of glycolysis with 2-DG caused a significant decrease in ATP levels, underscoring the contribution of residual glycolytic activity to maintain cellular ATP. In contrast, inhibition of OXPHOS with ORA or FCCP reduced total ATP levels to near-zero, indicating that spermatozoa increasingly rely on OXPHOS to sustain ATP levels when exogenous substrates are unavailable. Interestingly, sodium oxamate did not significantly reduce ATP levels under starving conditions, likely because

both glycolysis and OXPHOS can support basal ATP production from intracellular substrates, thereby maintaining minimal cellular energy homeostasis.

The proposed hypothesis of metabolic switching between glycolysis and OXPHOS necessitated direct measurement of ATP production rates supported by each pathway under different nutrient conditions. To address this, we performed Seahorse metabolic flux analysis, which revealed that media containing glucose (GLP, GL, GP, and G) consistently supported higher glycolytic ATP production rates than mitochondrial ATP production rates (Fig. 7). This observation is consistent with the predominantly glycolytic nature of human spermatozoa [8,35]. In contrast, total ATP production rates were significantly lower in glucose-free media (LP and O), with the majority of ATP in these conditions being generated via OXPHOS. Given that glycolysis accounted for nearly two-thirds of the total ATP production rate in glucose-containing media, it is reasonable to infer that glycolysis generates ATP at an approximately 36-fold higher rate than OXPHOS in human spermatozoa. However, surprisingly, the GLP medium did not support highest ATP production rate, despite consistently yielding the greatest degree of hyperactivation. Instead, Seahorse analysis indicated that GP or G media supported slightly higher ATP production rates than GLP, an observation that could not be readily explained. This discrepancy further reinforces the notion that hyperactivation depends not solely on total ATP production rates, but also on spatial regulation, metabolic coupling, and the efficiency of ATP delivery to the flagellum.

This spatial compartmentalization in sperm limits direct metabolic cross-talk between glycolysis and oxidative phosphorylation (OXPHOS), preventing these pathways from readily compensating for one another's energy demands [32,34,36]. Consequently, sperm energy metabolism is largely dictated by cellular architecture: glycolysis localized to the flagellum supplies ATP required for

motility, whereas mitochondria in the midpiece primarily support basal cellular metabolism [32,37]. It has also been proposed that mitochondrial ATP contributes to the initiation of the motility wave at the midpiece, which is subsequently propagated along the flagellum by ATP generated locally through glycolysis, thereby facilitating hyperactivated motility [38]. Regardless of the precise division of labor, accumulating evidence indicates that mitochondrial ATP alone cannot meet the energy demands along the entire length of the flagellum, necessitating localized glycolytic ATP production to sustain motility and hyperactivation [39–41]. Within this framework, pyruvate emerges as a critical metabolic enhancer, providing a "turbo" effect that amplifies glycolytic flux and supports hyperactivation, thereby underscoring its importance in male fertility [10].

Experimental interference with glycolysis completely abolishes sperm hyperactivation, whereas inhibition of oxidative phosphorylation (OXPHOS) significantly reduces hyperactivation but still permits a subset of spermatozoa to become hyperactivated. These findings suggest that targeting glycolysis may represent a more effective contraceptive strategy than inhibiting OXPHOS. Regarding the optimal point of intervention within the glycolytic pathway, inhibition of the initial step using 2-deoxyglucose (2-DG) or blockade of the anaerobic conversion of pyruvate to lactate via lactate dehydrogenase (LDH) appears similarly effective. This suggests that inhibition at multiple glycolytic steps may be equally promising, although this requires further validation using small-molecule inhibitors. Interestingly, a number of glycolytic enzymes exhibit sperm-specific isoforms, which can provide a safe approach targeting glycolysis for non-hormonal contraception. Supporting this concept, mouse knockout models for six of the seven glycolytic enzymes studied to date exhibit infertility. Occasional fertility observed in some knockout models may be

attributable to compensatory or alternative metabolic pathways that partially sustain glycolytic ATP production [19].

Conclusions

Human spermatozoa are metabolically adaptable cells capable of surviving on multiple energy substrates. However, survival and progressive motility alone are insufficient for fertilization; the ability to undergo hyperactivation is the defining determinant of sperm fertilizing potential. This study highlights several key conclusions. First, sperm hyperactivation is the most critical functional parameter for assessing fertility potential. Even sperm that successfully migrate to the site of fertilization will fail to fertilize the oocyte if they cannot achieve hyperactivation. Second, glycolytic ATP production is essential for inducing hyperactivation, and inhibition of glycolysis effectively suppresses this process under physiological conditions. Third, glucose availability is indispensable for hyperactivation, with pyruvate-to-lactate conversion providing a synergistic enhancement, likely by sustaining glycolytic flux. Fourth, oxidative phosphorylation (OXPHOS), while not absolutely essential, is not entirely dispensable even in nutrient-rich conditions. It plays a supportive role in maintaining optimal progressive motility and facilitating full hyperactivation. Notably, inhibition of OXPHOS does not abolish hyperactivation to the same extent as glycolytic blockade. Fifth, although sperm can maintain overall ATP levels through multiple metabolic pathways in enriched media, localized ATP production via glycolysis along the flagellum is crucial for driving hyperactivation. Collectively, these findings indicate that targeting glycolysis represents a more promising contraceptive strategy than inhibiting OXPHOS. Suppressing glycolysis can significantly impair sperm hyperactivation, even when progressive motility is preserved, thereby effectively reducing fertilization potential. In summary, glycolysis is

indispensable for sperm hyperactivation and fertility, whereas OXPHOS serves a complementary role by supporting motility and hyperactivation either through indirect cellular functions or limited ATP diffusion into the flagellum.

Declarations:

Ethics approval and consent to participate

The study was approved by the Institutional Human Ethics Committee of the Central Drug Research Institute, Lucknow (CDRI/IEC/2025/A1).

Consent for publication

The participants provided written consent for participation and publication of data.

Availability of data and materials

All data are available from authors with a reasonable request.

Competing interests

Authors have no conflict of interest to declare.

Funding

The study was funded by the Gates Foundation under grant number INV-062189.

Authors' contributions

MD, PK, BCN, SKB and RS performed experiments and analyzed data. All authors participated in writing of the article. RR and RS conceived the idea and secured funding.

Acknowledgements

The authors are thankful to anonymous semen donors without which the study would not have been possible.

Legends to figures

Fig. 1. Total motility, progressive motility, hyperactivated motility and mean curvilinear velocity under various substrate conditions in the human tubal fluid (HTF) medium. GLP; glucose, lactate, pyruvate, GP: glucose, pyruvate, GL; glucose, lactate, LP; lactate, pyruvate, O; no energy substrate added (basal HTF medium). All parameters were recorded every 10 minutes up to 60 minutes.

[*We calculated p-value using paired t-test for all the conditions at 60 minutes. We considered complete medium i.e., GLP as control and all the other conditions as cases. P-values for total motility were 0.0414(O), 0.278(G), 0.070(GP), 0.421(GL), 0.421(LP). P-values for progressive motility were 0.132(O), 0.295(G), 0.313(GP), 0.568(GL), 0.479(LP). P-values for hyperactivated motility were 0.012(O), 0.065(G), 0.778(GP), 0.039(GL), 0.043(LP). P-values for mean curvilinear velocity were, 0.008(O), 0.022(G), 0.492(GP), 0.029(GL), 0.049(LP).*]

Fig. 2. Total motility, progressive motility, hyperactivated motility and mean curvilinear velocity under various substrate conditions in the human tubal fluid (HTF) medium. GLP; glucose, lactate, pyruvate, GP: glucose, pyruvate, GL; glucose, lactate, LP; lactate, pyruvate, O; no energy substrate added (basal HTF medium). All parameters were recorded at 1, 3, 6, 18, and 24 hours.

Fig. 3. Total motility, progressive motility, hyperactivated motility and mean curvilinear velocity in the presence of 2-DG in the full HTF (with glucose, lactate, pyruvate) and O (basal HTF without energy substrates) medium. All parameters were recorded every 10 minutes up to 60 minutes.

[*We calculated p-value using paired t-test for all the conditions at 60 minutes. We compared O and GLP conditions separately with their respective inhibitor conditions. P-values for total motility against O & GLP medium were 0.024 (O-2DG10mM) and 0.056 (O-2DG25mM) & 0.125 (GLP-2DG10mM) and 0.101 (GLP-2DG25mM), respectively. P-values for progressive motility against O & GLP medium were 0.0002 (O-2DG10mM) and 0.0001(O-2DG25mM) & 0.586 (GLP-2DG10mM) and 0.128 (GLP-2DG25mM), respectively. P-values for hyperactivated motility against O &*

GLP medium were 0.037 (O-2DG10mM) and 0.014 (O-2DG25mM) & 0.0.0001(GLP-2DG10mM) and 0.0001(GLP-2DG25mM), respectively. P-values for curvilinear velocity against O & GLP medium were 0.043 (O-2DG10mM) and 0.009(O-2DG25mM) & 0.005 (GLP-2DG10mM) and 0.0003(GLP-2DG25mM), respectively].

Fig. 4. Total motility, progressive motility, hyperactivated motility and mean curvilinear velocity in the presence of sodium oxamate in the full HTF (with glucose, lactate and pyruvate) and O (basal HTF without energy substrates) medium. All parameters were recorded every 10 minutes up to 60 minutes.

[*We calculated p-value using paired t-test for all the conditions at 60th minute. We compared O and GLP conditions separately with their respective inhibitor conditions. The calculated p-values for total motility against O & GLP medium are 0.006 (O-ox50uM) and 0.004 (O-ox100uM) & 0.016(GLP-Ox50uM) and 0.0001(GLP-Ox100uM), respectively. The calculated p-values for progressive motility against O & GLP medium were 0.037 (O-Ox50uM) and 0.001(O-Ox100uM) & 0.0002 (GLP-Ox50uM) and 0.0001 (GLP-Ox100uM), respectively. The calculated p-values for hyperactivated motility against O & GLP medium were 0.999 (O-Ox50uM) and 0.765 (O-Ox100uM) & 0.0001(GLP-Ox50uM) and 0.0001(GLP-Ox100uM), respectively. The calculated p-values for mean curvilinear velocity against O & GLP medium were 0.042 (O-Ox50uM) and 0.008 (O-Ox100uM) & 0.0001 (GLP-Ox50uM) and 0.0001 (GLP-Ox100uM), respectively.*]

Fig. 5. Total motility, progressive motility, hyperactivated motility and mean curvilinear velocity in the presence of OXPHOS inhibitors (oligomycin, rotenone and antimycin A, ORA) in the full HTF (with glucose, lactate and pyruvate) and O (basal HTF without energy substrates) medium. All parameters were recorded every 10 minutes up to 60 minutes.

[*We calculated p-value using paired t-test for all the conditions at 60th minute. We compared O and GLP conditions separately with their respective inhibitor conditions. The calculated p-values for total motility against O & GLP medium were 0.0001 (O-ORA1X) and 0.0004 (GLP-ORA1X), respectively. The calculated p-values for progressive*

motility against O & GLP medium were 0.0001 (O-ORA1X) and 0.004 (GLP-ORA1X), respectively. The calculated p-values for hyperactivated motility against O & GLP medium were 0.025 (O-ORA1X) and 0.005 (GLP-ORA1X), respectively. The calculated p-values for mean curvilinear velocity against O & GLP medium were 0.0001 (O-ORA1X) and 0.002 (GLP-ORA1X), respectively.]

Fig. 6. Total motility, progressive motility, hyperactivated motility and mean curvilinear velocity in the presence of OXPHOS uncoupler (FCCP) in the full HTF (with glucose, lactate and pyruvate) and O (basal HTF without energy substrates) medium. All parameters were recorded every 10 minutes up to 60 minutes.

[*We calculated p-value using paired t-test for all the conditions at 60th minute. We compared O and GLP conditions separately with their respective inhibitor conditions. The calculated p-values for total motility against O & GLP medium are 0.012 (O-FCCP) and 0.227 (GLP-FCCP), respectively. The calculated p-values for progressive motility against O & GLP medium were 0.061 (O-FCCP) and 0.689 (GLP-FCCP), respectively. The calculated p-values for hyperactivated motility against O & GLP medium were 0.205 (O-FCCP) and 0.013 (GLP-FCCP), respectively. The calculated p-values for mean curvilinear velocity against O & GLP medium were 0.0003 (O-FCCP) and 0.014 (GLP-FCCP), respectively.*]

Fig. 7. Intracellular ATP concentration per 20 million sperm (upper panel) and ATP production rate by glycolysis and OXPHOS per million sperm (lower panel) in the presence of various substrates in the basal HTF (O) medium.

Fig. 8. Upper panel; Intracellular sperm ATP concentration per 20 million sperm in the presence of glycolytic inhibitors (2-DG and oxamate) and OXPHOS inhibitors (oligomycin, rotenone and antimycin A, ORA and FCCP) in the full GLP and O (basal) media, and lower panel; ATP production rate per million sperm from glycolysis and OXPHOS in the presence of glycolytic inhibitors (2-DG and oxamate) in the full GLP and O (basal) media.

[*We calculated p-value using paired t-test for all the conditions at 60 minutes. We compared O and GLP conditions separately with their respective inhibitor conditions. The calculated p-values for intracellular ATP production against O medium were 0.019 (DG10mM), 0.785 (Ox50mM), 0.341 (ORA1x) and 0.026 (FCCP5uM). The calculated p-values for intracellular ATP production against GLP medium were 0.0013 (DG10mM), 0.199 (Ox50mM), 0.462 (ORA1x) and 0.172 (FCCP5uM).*]

Supplementary Figures

Supplementary Fig. 1. Vitality assay for sperm cells suspended in the HTF medium with different energy substrates (GLP, GP, GL, LP, G, O) up to 24 hours.

Supplementary Fig. 2. Vitality assay for sperm cells suspended in the HTF (GLP and O) medium with different inhibitors (2-DG, sodium oxamate, ORA, FCCP) up to 60 minutes.

Supplementary Fig. 3. Seahorse assay OCR and ECAR values in modified PBS with different energy substrates (GLP, GP, GL, LP, G and O).

Supplementary Fig. 4. Seahorse assay OCR and ECAR values in modified PBS (GLP and O) with glycolytic inhibitors (2-DG and sodium oxamate).

Supplementary Fig. 5. Sperm motility patterns captured at 60 minutes using CASA under various substrate conditions.

Supplementary Fig 6. Sperm motility patterns captured at 60 minutes using CASA in the presence of 2DG in HTF GLP and O media.

Supplementary Fig. 7. Sperm motility patterns captured at 60 minutes using CASA in the presence of sodium oxamate in HTF GLP and O media.

Supplementary Fig. 8. Sperm motility patterns captured at 60 minutes using CASA in the presence of ORA and FCCP in HTF GLP and O media.

References

1. Balbach M, Rossetti T, Ferreira J, Ghanem L, Ritagliati C, Myers RW, et al. On-demand male contraception via acute inhibition of soluble adenylyl cyclase. Nat Commun. 2023;14:637. https://doi.org/10.1038/s41467-023-36119-6

2. Balbach M, Ghanem L, Rossetti T, Kaur N, Ritagliati C, Ferreira J, et al. Soluble adenylyl cyclase inhibition prevents human sperm functions essential for fertilization. Mol Hum Reprod. 2021;27:gaab054. https://doi.org/10.1093/molehr/gaab054

3. Ferreira J, Levin LR, Buck J. Strategies to safely target widely expressed soluble adenylyl cyclase for contraception. Front Pharmacol. 2022;13:953903. https://doi.org/10.3389/fphar.2022.953903

4. Silva EJR, Hamil KG, Richardson RT, O'Rand MG. Characterization of EPPIN's semenogelin I binding site: a contraceptive drug target. Biol Reprod. 2012;87:56. https://doi.org/10.1095/biolreprod.112.101832

5. Goodson SG, Qiu Y, Sutton KA, Xie G, Jia W, O'Brien DA. Metabolic Substrates Exhibit Differential Effects on Functional Parameters of Mouse Sperm Capacitation1. Biol Reprod. 2012;87:75. https://doi.org/10.1095/biolreprod.112.102673

6. Darr CR, Varner DD, Teague S, Cortopassi GA, Datta S, Meyers SA. Lactate and Pyruvate Are Major Sources of Energy for Stallion Sperm with Dose Effects on Mitochondrial Function, Motility, and ROS Production. Biol Reprod. 2016;95:34. https://doi.org/10.1095/biolreprod.116.140707

7. Hossain MMF, Yamanaka T, Shahrina A, Koyago M, Shimada M. Lactate inhibits glucose-induced zigzag motility and enhances linear motility in bull spermatozoa by suppressing glycolysis. Andrology. 2025; https://doi.org/10.1111/andr.70113

8. Balbach M, Ghanem L, Violante S, Kyaw A, Romarowski A, Cross JR, et al. Capacitation induces changes in metabolic pathways supporting motility of epididymal and ejaculated sperm. Front Cell Dev Biol. 2023;11:1160154. https://doi.org/10.3389/fcell.2023.1160154

9. Carrageta DF, Guerra-Carvalho B, Sousa M, Barros A, Oliveira PF, Monteiro MP, et al. Mitochondrial Activation and Reactive Oxygen-Species Overproduction during Sperm Capacitation are Independent of Glucose Stimuli. Antioxidants [Internet]. publisher; 2020 [cited 2025 Nov 13];9. https://doi.org/10.3390/antiox9080750

10. Hereng TH, Elgstøen KBP, Cederkvist FH, Eide L, Jahnsen T, Skålhegg BS, et al. Exogenous pyruvate accelerates glycolysis and promotes capacitation in human spermatozoa. Hum Reprod. 2011;26:3249–63. https://doi.org/10.1093/humrep/der317

11. Marín-Briggiler CI, Luque GM, Gervasi MG, Oscoz-Susino N, Sierra JM, Mondillo C, et al. Human Sperm Remain Motile After a Temporary Energy Restriction but do Not Undergo Capacitation-Related Events. Front Cell Dev Biol [Internet]. Frontiers; 2021 [cited 2025 Nov 13];9. https://doi.org/10.3389/fcell.2021.777086

12. Storey BT. Mammalian sperm metabolism: oxygen and sugar, friend and foe. Int J Dev Biol. 2008;52:427–37. https://doi.org/10.1387/ijdb.072522bs

13. Miki K, Qu W, Goulding EH, Willis WD, Bunch DO, Strader LF, et al. Glyceraldehyde 3-phosphate dehydrogenase-S, a sperm-specific glycolytic enzyme, is required for sperm motility and male fertility. Proc Natl Acad Sci U S A. 2004;101:16501–6. https://doi.org/10.1073/pnas.0407708101

14. Nakamura N, Dai Q, Williams J, Goulding EH, Willis WD, Brown PR, et al. Disruption of a spermatogenic cell-specific mouse enolase 4 (eno4) gene causes sperm structural defects and male infertility. Biol Reprod. 2013;88:90. https://doi.org/10.1095/biolreprod.112.107128

15. Odet F, Duan C, Willis WD, Goulding EH, Kung A, Eddy EM, et al. Expression of the gene for mouse lactate dehydrogenase C (Ldhc) is required for male fertility. Biol Reprod. 2008;79:26–34. https://doi.org/10.1095/biolreprod.108.068353

16. Qian G-Q, Wang X-C, Zhang X, Shen B, Liu Q. Pyruvate kinase M in germ cells is essential for sperm motility and male fertility but not spermatogenesis. Asian J Androl. 2024;26:212–9. https://doi.org/10.4103/aja202350

17. Tian Y, Chen X, Pu J, Liang Y, Li W, Xu X, et al. Spermatogenic cell-specific type 1 hexokinase (HK1S) is essential for capacitation-associated increase in tyrosine phosphorylation and male fertility in mice. PLoS Genet. 2024;20:e1011357. https://doi.org/10.1371/journal.pgen.1011357

18. Noda T, Taira A, Shinohara H, Araki K. The testis-, epididymis-, or seminal vesicle-enriched genes Aldoart2, Serpina16, Aoc1l3, and Pate14 are not essential for male fertility in mice. Exp Anim. 2023;72:314–23. https://doi.org/10.1538/expanim.22-0158

19. Danshina PV, Geyer CB, Dai Q, Goulding EH, Willis WD, Kitto GB, et al. Phosphoglycerate kinase 2 (PGK2) is essential for sperm function and male fertility in mice. Biol Reprod. 2010;82:136–45. https://doi.org/10.1095/biolreprod.109.079699

20. Freundl G, Grimm HJ, Hofmann N. Selective filtration of abnormal spermatozoa by the cervical mucus*. Hum Reprod. 1988;3:277–80. https://doi.org/10.1093/oxfordjournals.humrep.a136695

21. Lee M, Park JW, Kim D, Kwon H, Cho MJ, Lee EJ, et al. Viscous Cervical Environment-on-a-Chip for Selecting High-Quality Sperm from Human Semen. Biomedicines. 2021;9:1439. https://doi.org/10.3390/biomedicines9101439

22. Ferramosca A, Zara V. Bioenergetics of Mammalian Sperm Capacitation. Biomed Res Int. 2014;2014:902953. https://doi.org/10.1155/2014/902953

23. Suarez SS. Control of hyperactivation in sperm. Hum Reprod Update. 2008;14:647–57. https://doi.org/10.1093/humupd/dmn029

24. Ferreira-Poblete A. The probability of conception on different days of the cycle with respect to ovulation: an overview. Adv Contracept. 1997;13:83–95. https://doi.org/10.1023/a:1006527232605

25. Suarez SS, Pacey AA. Sperm transport in the female reproductive tract. Hum Reprod Update. 2006;12:23–37. https://doi.org/10.1093/humupd/dmi047

26. Akthar I, Yousef MS, Mansouri A, Shimada M, Miyamoto A. Sperm hyperactivation in the uterus and oviduct: a double-edged sword for sperm and maternal innate immunity toward fertility. Animal Reproduction. 2024;21:e20240043. https://doi.org/10.1590/1984-3143-AR2024-0043

27. Mortimer ST, Swan MA, Mortimer D. Effect of seminal plasma on capacitation and hyperactivation in human spermatozoa. Human Reproduction. 1998;13:2139–46. https://doi.org/10.1093/humrep/13.8.2139

28. WHO laboratory manual for the examination and processing of human semen [Internet]. World Health Organization; 2021 [cited 2026 Jan 27]. https://www.who.int/publications/b/59107. Accessed 27 Jan 2026

29. Balbach M, Gervasi MG, Hidalgo DM, Visconti PE, Levin LR, Buck J. Metabolic changes in mouse sperm during capacitation. Biol Reprod. 2020;103:791–801. https://doi.org/10.1093/biolre/ioaa114

30. Lodge JR, Harms PG, Graves CN. Effect of 2-Deoxyglucose on Bovine Spermatozoan Metabolism and Preservation. Journal of Dairy Science. 1968;51:1085–90. https://doi.org/10.3168/jds.S0022-0302(68)87129-2

31. Duan C, Goldberg E. Inhibition of lactate dehydrogenase C4 (LDH-C4) blocks capacitation of mouse sperm in vitro. Cytogenet Genome Res. 2004;103:352–9. https://doi.org/10.1159/000076824

32. Amaral A. Energy metabolism in mammalian sperm motility. WIREs Mech Dis. 2022;14:e1569. https://doi.org/10.1002/wsbm.1569

33. Kipnis DM, Cori CF. Studies of tissue permeability. III. The effect of insulin on pentose uptake by the diaphragm. J Biol Chem. 1957;224:681–93.

34. Visconti PE. Sperm Bioenergetics in a Nutshell1. Biol Reprod. 2012;87:72. https://doi.org/10.1095/biolreprod.112.104109

35. Freitas-Martins A, Sousa MI, Cristo MI, Ramalho-Santos J, Amaral S. Metabolic characterization of human sperm cells using the Seahorse metabolic flux analyzer. Andrology. 2024;12:410–21. https://doi.org/10.1111/andr.13486

36. Park Y-J, Pang M-G. Mitochondrial Functionality in Male Fertility: From Spermatogenesis to Fertilization. Antioxidants (Basel). 2021;10:98. https://doi.org/10.3390/antiox10010098

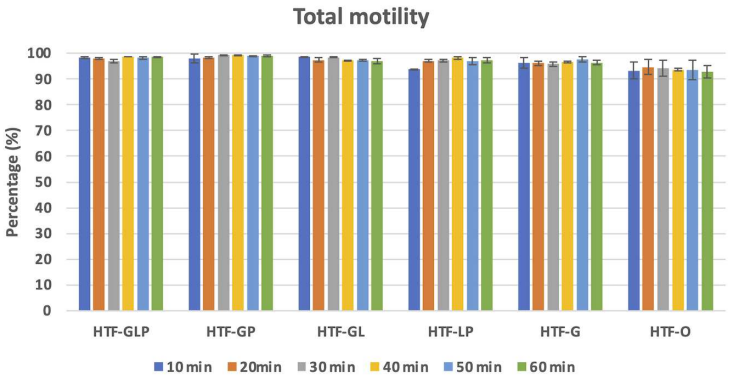
37. Naletova I, Schmalhausen E, Tomasello B, Pozdyshev D, Attanasio F, Muronetz V. The role of sperm-specific glyceraldehyde-3-phosphate dehydrogenase in the development of pathologies—from asthenozoospermia to carcinogenesis. Front Mol Biosci [Internet]. Frontiers; 2023 [cited 2025 Nov 13];10. https://doi.org/10.3389/fmolb.2023.1256963

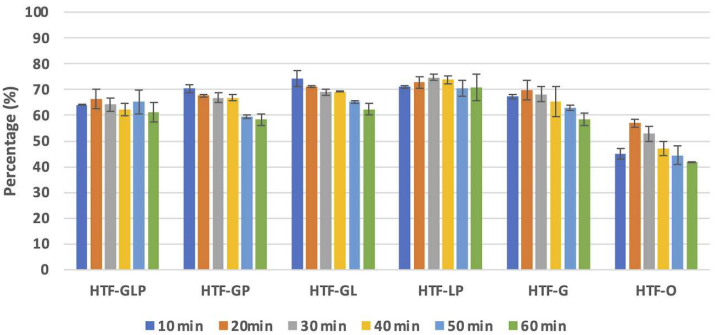
38. Sansegundo E, Tourmente M, Roldan ERS, Sansegundo E, Tourmente M, Roldan ERS. Energy Metabolism and Hyperactivation of Spermatozoa from Three Mouse Species under Capacitating Conditions. Cells [Internet]. publisher; 2022 [cited 2025 Nov 13];11. https://doi.org/10.3390/cells11020220

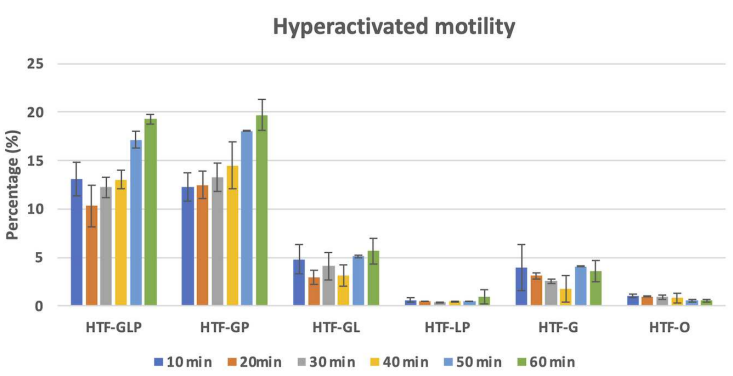
39. du Plessis SS, Agarwal A, Mohanty G, van der Linde M. Oxidative phosphorylation versus glycolysis: what fuel do spermatozoa use? Asian J Androl. 2015;17:230–5. https://doi.org/10.4103/1008-682X.135123

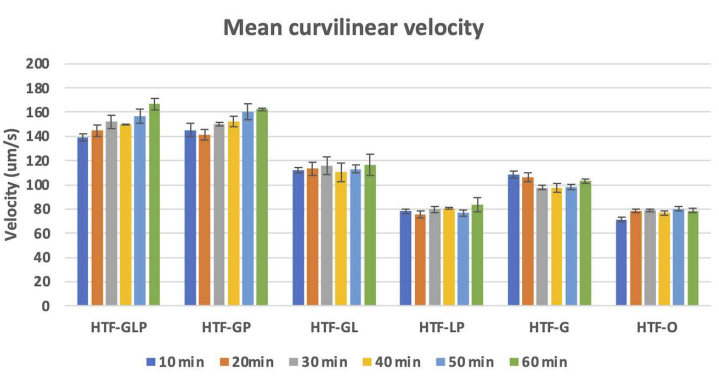
40. Ford WCL. Glycolysis and sperm motility: does a spoonful of sugar help the flagellum go round? Hum Reprod Update. 2006;12:269–74. https://doi.org/10.1093/humupd/dmi053

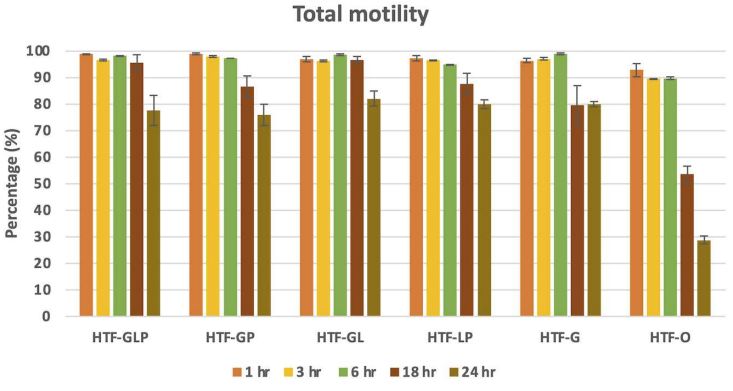
41. Tourmente M, Sansegundo E, Rial E, Roldan ERS. Capacitation promotes a shift in energy metabolism in murine sperm. Front Cell Dev Biol [Internet]. Frontiers; 2022 [cited 2025 Nov 13];10. https://doi.org/10.3389/fcell.2022.950979

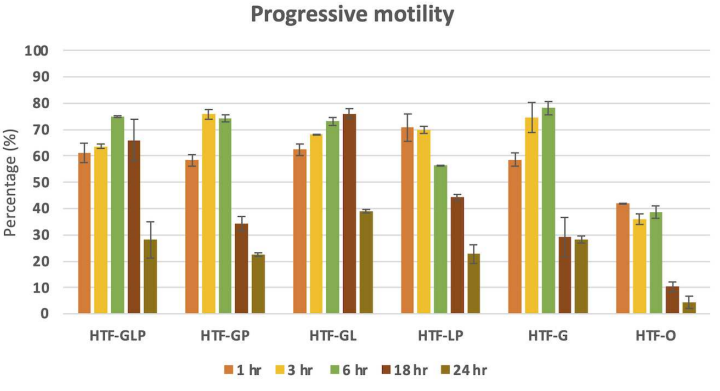

Total motility
Percentage (%)
100
90
80
70
60
50
40
30
20
10
0
HTF-GLP
HTF-GP
HTF-GL
HTF-LP
HTF-G
HTF-O
10 min
20min
30 min
40 min
50 min
60 min

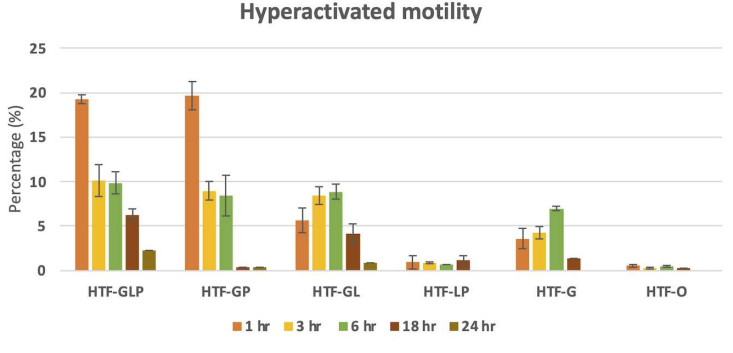

Progressive motility
Percentage (%)
100
90
80
70
60
50
40
30
20
10
0
HTF-GLP
HTF-GP
HTF-GL
HTF-LP
HTF-G
HTF-O
10 min
20min
30 min
40 min
50 min
60 min

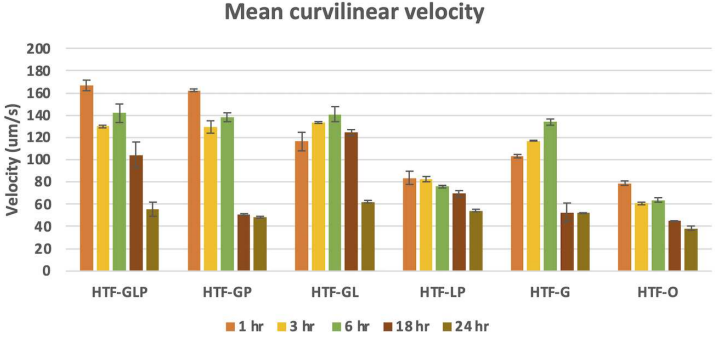

Hyperactivated motility
Percentage (%)
25
20
15
10
5
0
HTF-GLP
HTF-GP
HTF-GL
HTF-LP
HTF-G
HTF-O
10 min
20min
30 min
40 min
50 min
60 min

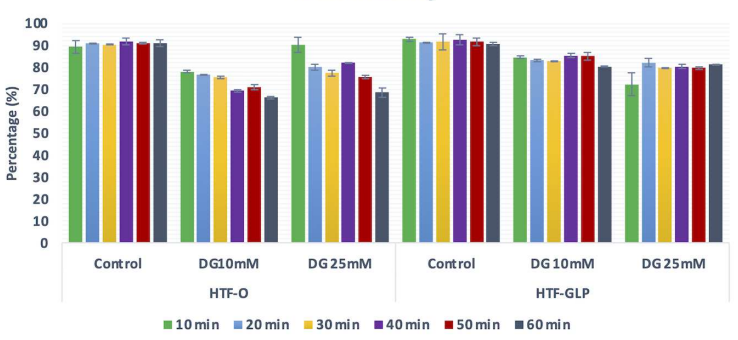

Mean curvilinear velocity
Velocity (um/s)
200
180
160
140
120
100
80
60
40
20
0
HTF-GLP
HTF-GP
HTF-GL
HTF-LP
HTF-G
HTF-O
10 min
20min
30 min
40 min
50 min
60 min

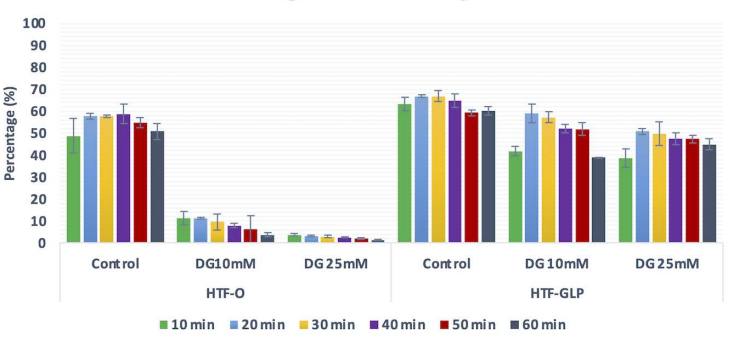

Total motility
Percentage (%)
100
90
80
70
60
50
40
30
20
10
0
HTF-GLP
HTF-GP
HTF-GL
HTF-LP
HTF-G
HTF-O
1 hr
3 hr
6 hr
18 hr
24 hr

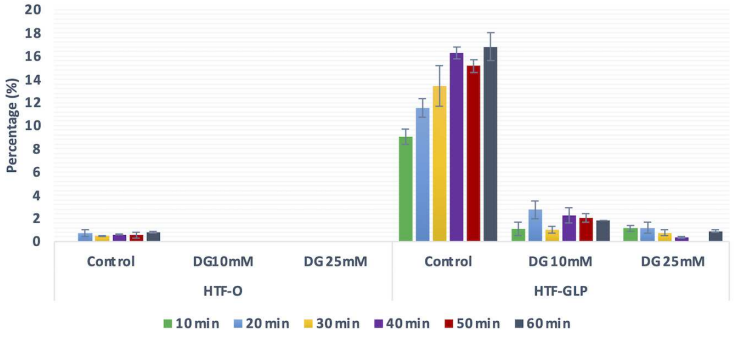

Progressive motility
Percentage (%)
100
90
80
70
60
50
40
30
20
10
0
HTF-GLP
HTF-GP
HTF-GL
HTF-LP
HTF-G
HTF-O
1 hr
3 hr
6 hr
18 hr
24 hr

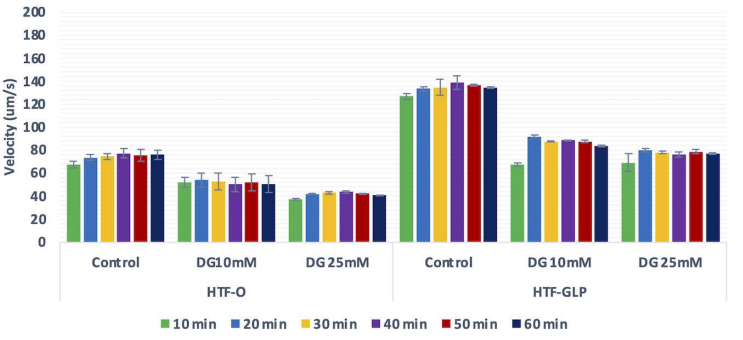

Hyperactivated motility
Percentage (%)
25
20
15
10
5
0
HTF-GLP
HTF-GP
HTF-GL
HTF-LP
HTF-G
HTF-O
1 hr
3 hr
6 hr
18 hr
24 hr


Mean curvilinear velocity
Velocity (um/s)
200
180
160
140
120
100
80
60
40
20
0
HTF-GLP
HTF-GP
HTF-GL
HTF-LP
HTF-G
HTF-O
1 hr
3 hr
6 hr
18 hr
24 hr

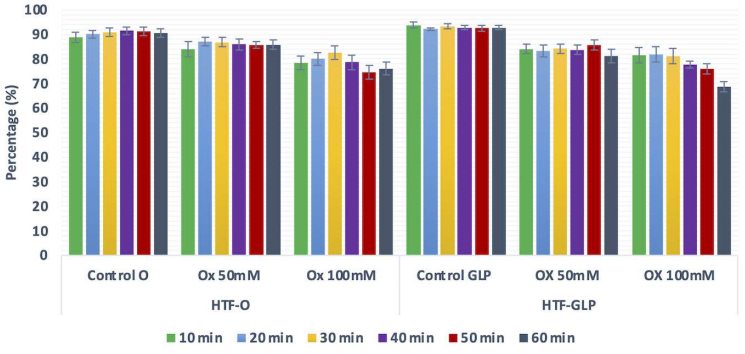

Total motility
Percentage (%)
100
90
80
70
60
50
40
30
20
10
0
Control
DG10mM
DG25mM
Control
DG10mM
DG25mM
HTF-O
HTF-GLP
10 min
20 min
30 min
40 min
50 min
60 min


Progressive motility
Percentage (%)
100
90
80
70
60
50
40
30
20
10
0
Control
DG10mM
DG25mM
Control
DG10mM
DG25mM
HTF-O
HTF-GLP
10 min
20 min
30 min
40 min
50 min
60 min

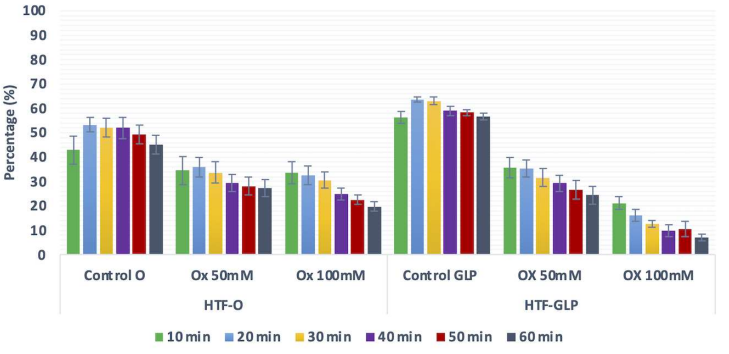

Hyperactivated motility
Percentage (%)
20
18
16
14
12
10
8
6
4
2
0
Control
DG10mM
DG25mM
Control
DG10mM
DG25mM
HTF-O
HTF-GLP
10 min
20 min
30 min
40 min
50 min
60 min


Mean curvilinear velocity
Velocity (um/s)
200
180
160
140
120
100
80
60
40
20
0
Control
DG10mM
DG25mM
Control
DG10mM
DG25mM
HTF-O
HTF-GLP
10 min
20 min
30 min
40 min
50 min
60 min

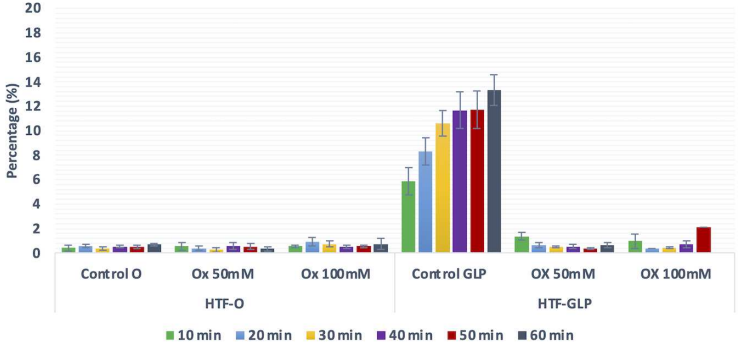
Total motility



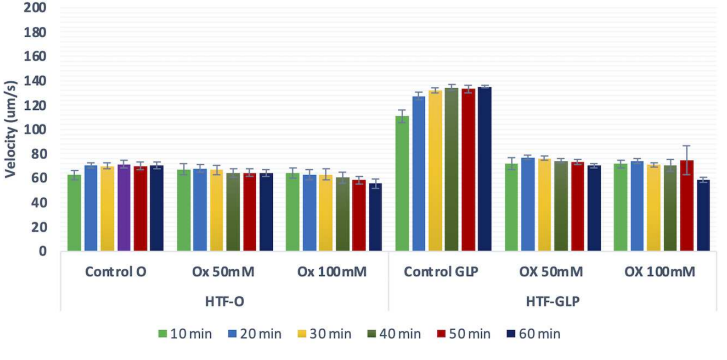
Progressive motility

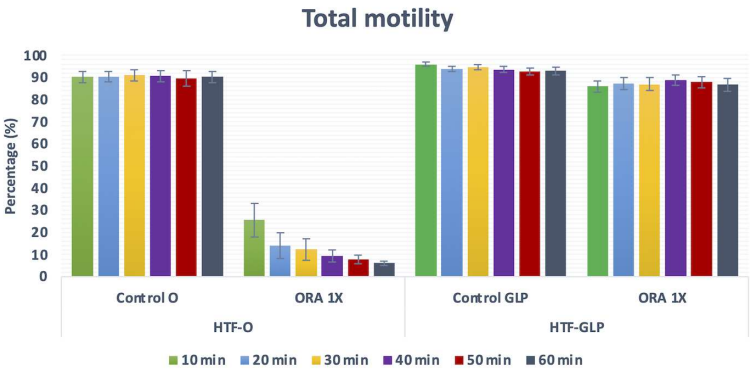


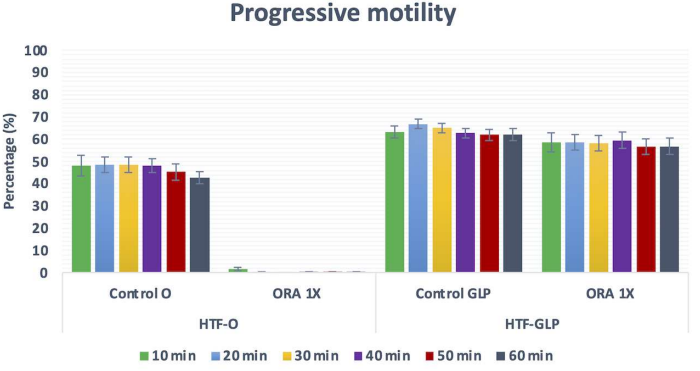
Hyperactivated motility

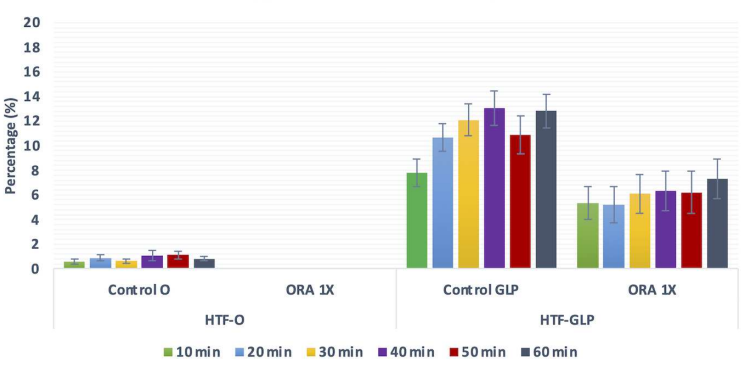


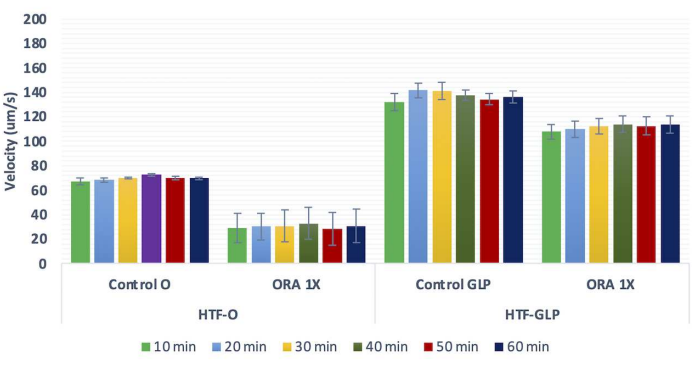
Mean curvilinear velocity

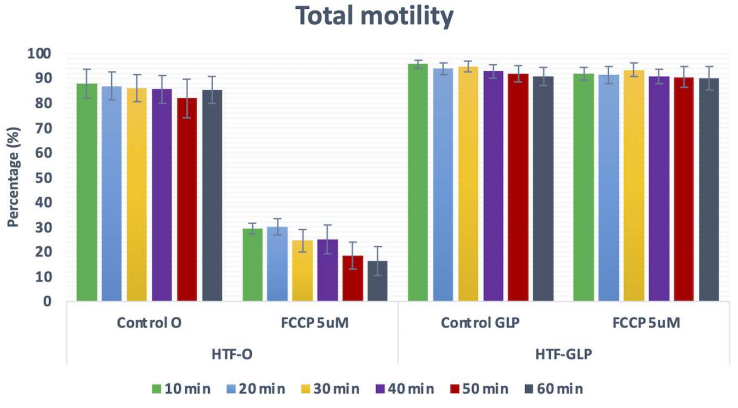


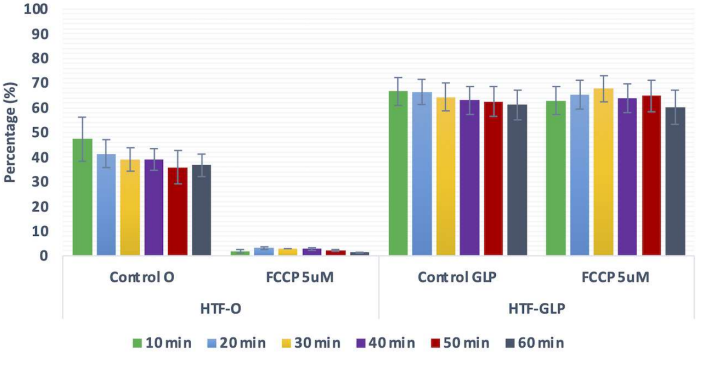

Total motility
Percentage (%)
100
90
80
70
60
50
40
30
20
10
0
Control O
ORA 1X
Control GLP
ORA 1X
HTF-O
HTF-GLP
10 min
20 min
30 min
40 min
50 min
60 min

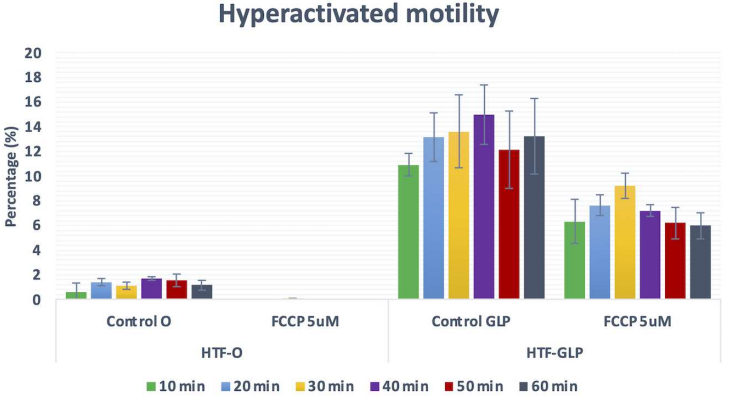

Progressive motility
Percentage (%)
100
90
80
70
60
50
40
30
20
10
0
Control O
ORA 1X
Control GLP
ORA 1X
HTF-O
HTF-GLP
10 min
20 min
30 min
40 min
50 min
60 min

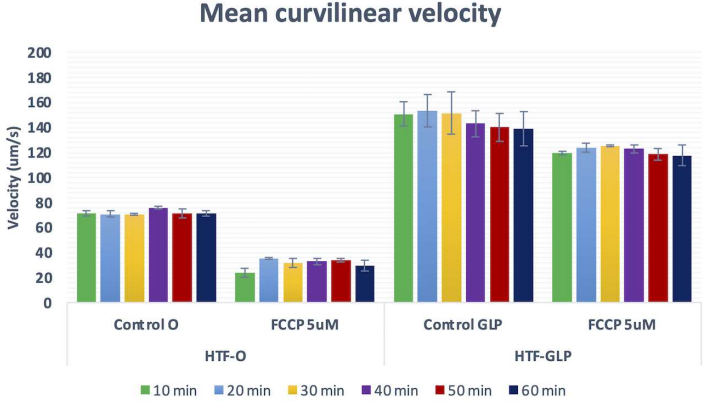

Hyperactivated motility
Percentage (%)
20
18
16
14
12
10
8
6
4
2
0
Control O
ORA 1X
Control GLP
ORA 1X
HTF-O
HTF-GLP
10 min
20 min
30 min
40 min
50 min
60 min

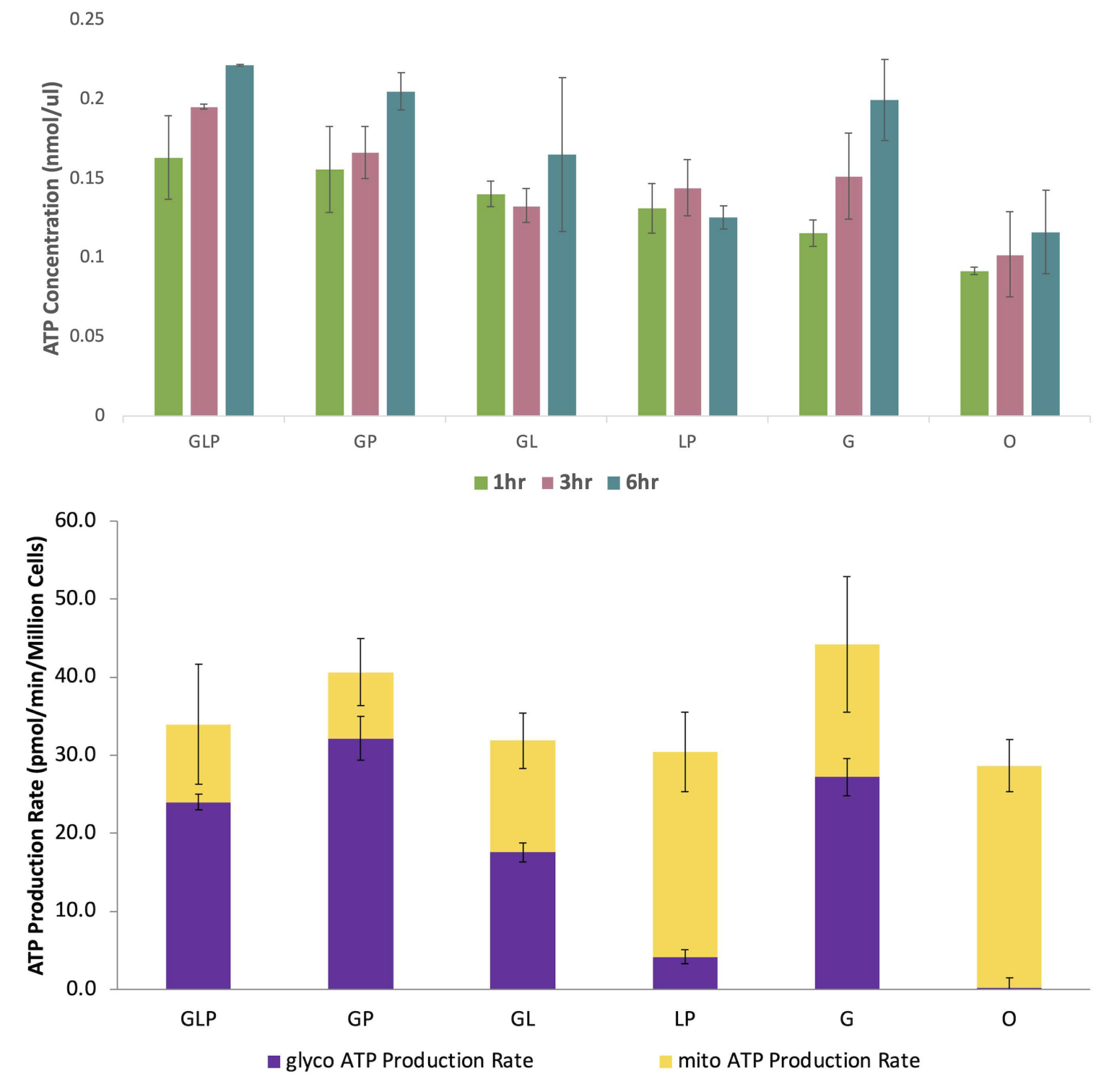

Mean curvilinear velocity
Velocity (um/s)
200
180
160
140
120
100
80
60
40
20
0
Control O
ORA 1X
Control GLP
ORA 1X
HTF-O
HTF-GLP
10 min
20 min
30 min
40 min
50 min
60 min

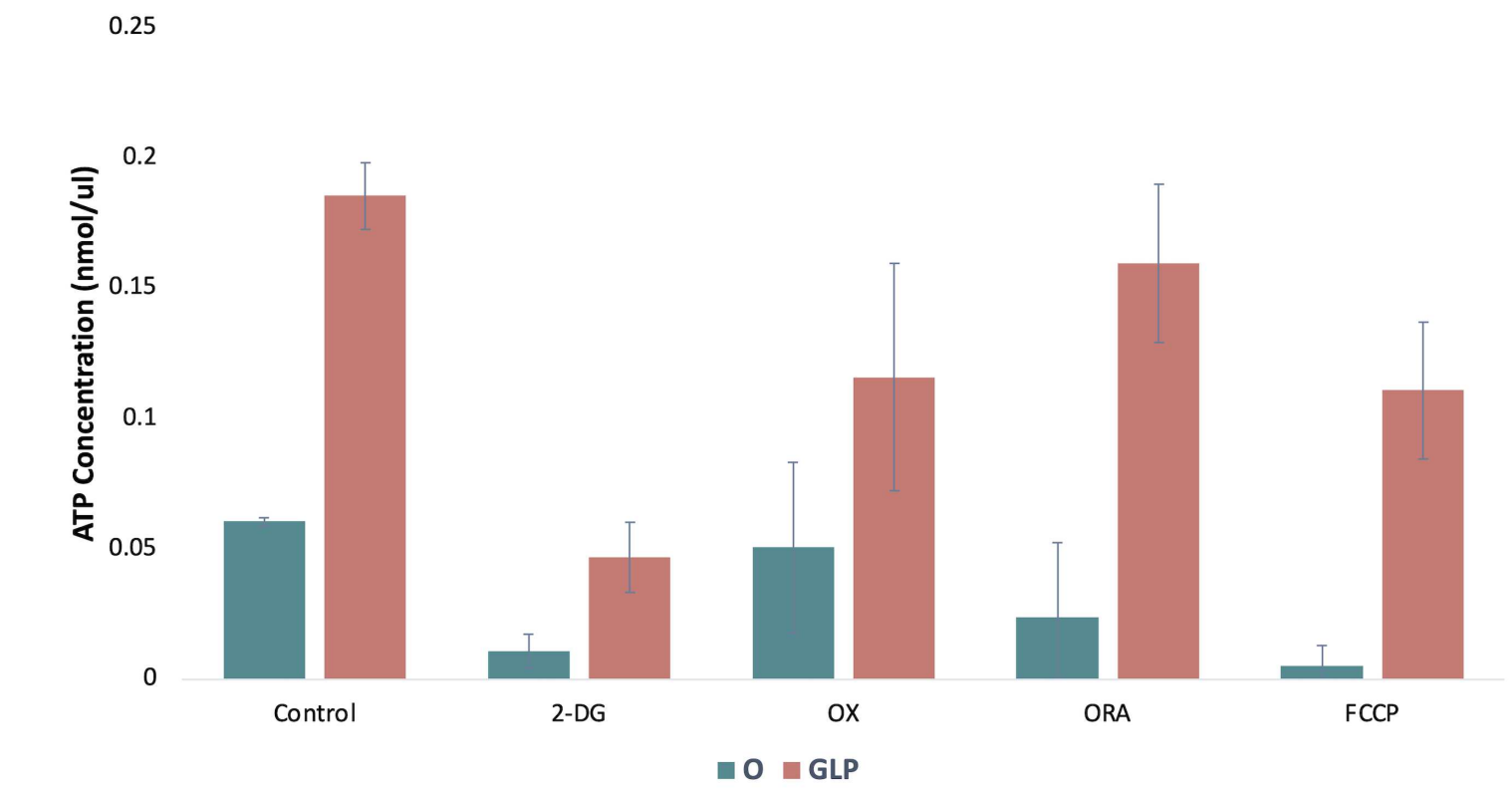

Total motility
Percentage (%)
100
90
80
70
60
50
40
30
20
10
0
Control O
FCCP 5uM
Control GLP
FCCP 5uM
HTF-O
HTF-GLP
10 min
20 min
30 min
40 min
50 min
60 min

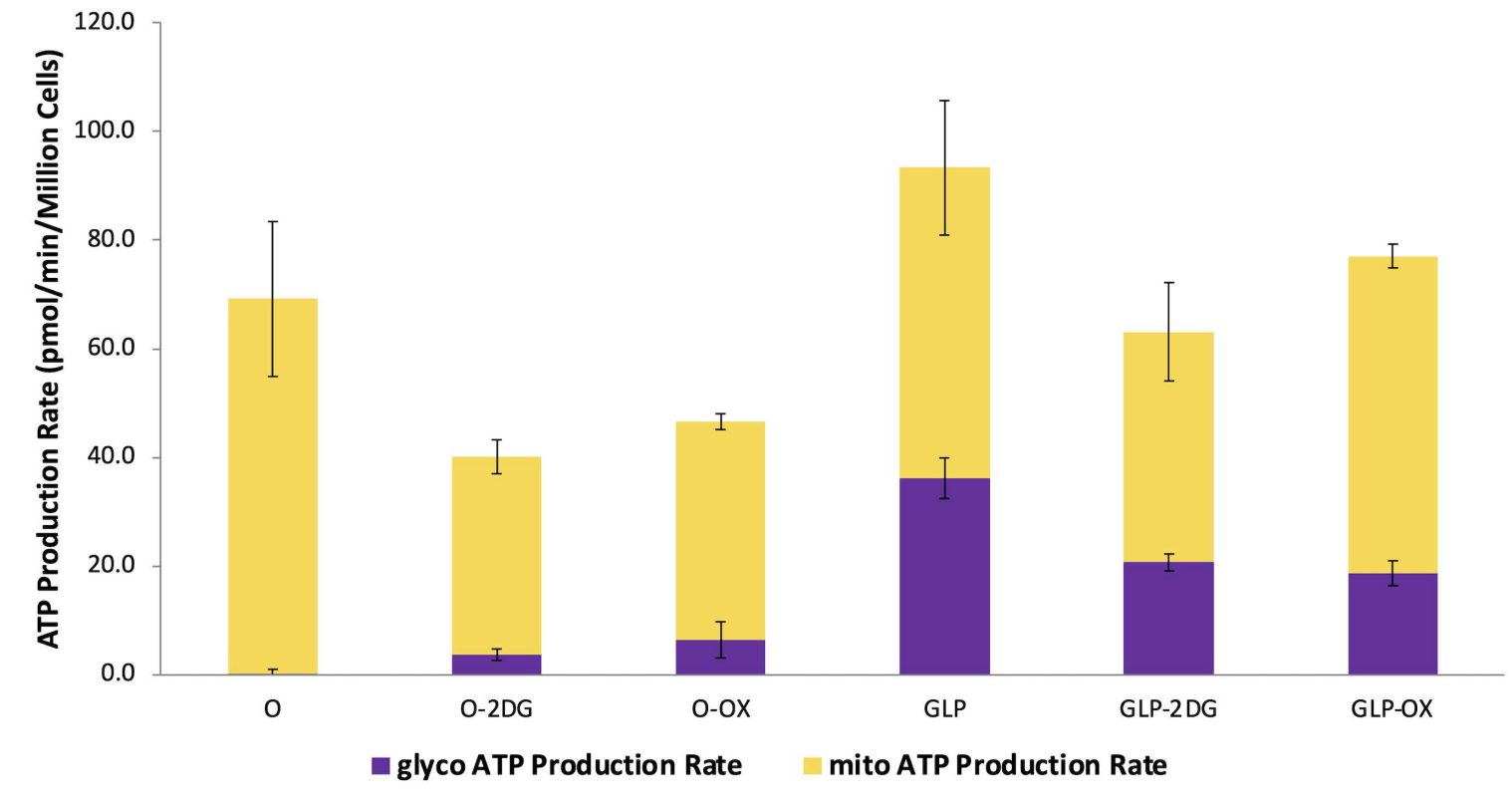

Progressive motility
Percentage (%)
100
90
80
70
60
50
40
30
20
10
0
Control O
FCCP 5uM
Control GLP
FCCP 5uM
HTF-O
HTF-GLP
10 min
20 min
30 min
40 min
50 min
60 min


Hyperactivated motility
Percentage (%)
20
18
16
14
12
10
8
6
4
2
0
Control O
FCCP 5uM
Control GLP
FCCP 5uM
HTF-O
HTF-GLP
10 min
20 min
30 min
40 min
50 min
60 min


Mean curvilinear velocity
Velocity (um/s)
200
180
160
140
120
100
80
60
40
20
0
Control O
FCCP 5uM
Control GLP
FCCP 5uM
HTF-O
HTF-GLP
10 min
20 min
30 min
40 min
50 min
60 min


ATP Concentration (nmol/ul)
0.25
0.2
0.15
0.1
0.05
0
GLP
GP
GL
LP
G
O
1hr
3hr
6hr
ATP Production Rate (pmol/min/Million Cells)
60.0
50.0
40.0
30.0
20.0
10.0
0.0
GLP
GP
GL
LP
G
O
glyco ATP Production Rate
mito ATP Production Rate


0.25
0.2
0.15
0.1
0.05
0
ATP Concentration (nmol/ul)
Control
2-DG
OX
ORA
FCCP
O
GLP


120.0
100.0
80.0
60.0
40.0
20.0
0.0
ATP Production Rate (pmol/min/Million Cells)
O
O-2DG
O-OX
GLP
GLP-2DG
GLP-OX
glyco ATP Production Rate
mito ATP Production Rate

Supplementary Files

This is a list of supplementary files associated with this preprint. Click to download.

- Supplementarymaterial.docx